Modulating the electronic structure of a hydrogen-bonded organic framework to improve the uranium removal by enhancing hydrogen evolution reaction

Qingsong Zhang [a, *], Yuyang Miao [a], Yang Xiao [b, *], Jianwei Hu [a], Haiyi Gong [a], Qingyi Zeng [a, *]

[a] School of Resource & Environment and Safety Engineering, University of South China, Hengyang 421001, China

[b] School of Nuclear Science and Technology, University of South China, Hengyang 421001, China

* Corresponding authors.
E-mail addresses: qszhang@usc.edu.cn (QS. Zhang); xiaoyang950529@163.com (Y. Xiao); qingyizeng@usc.edu.cn (QY. Zeng)

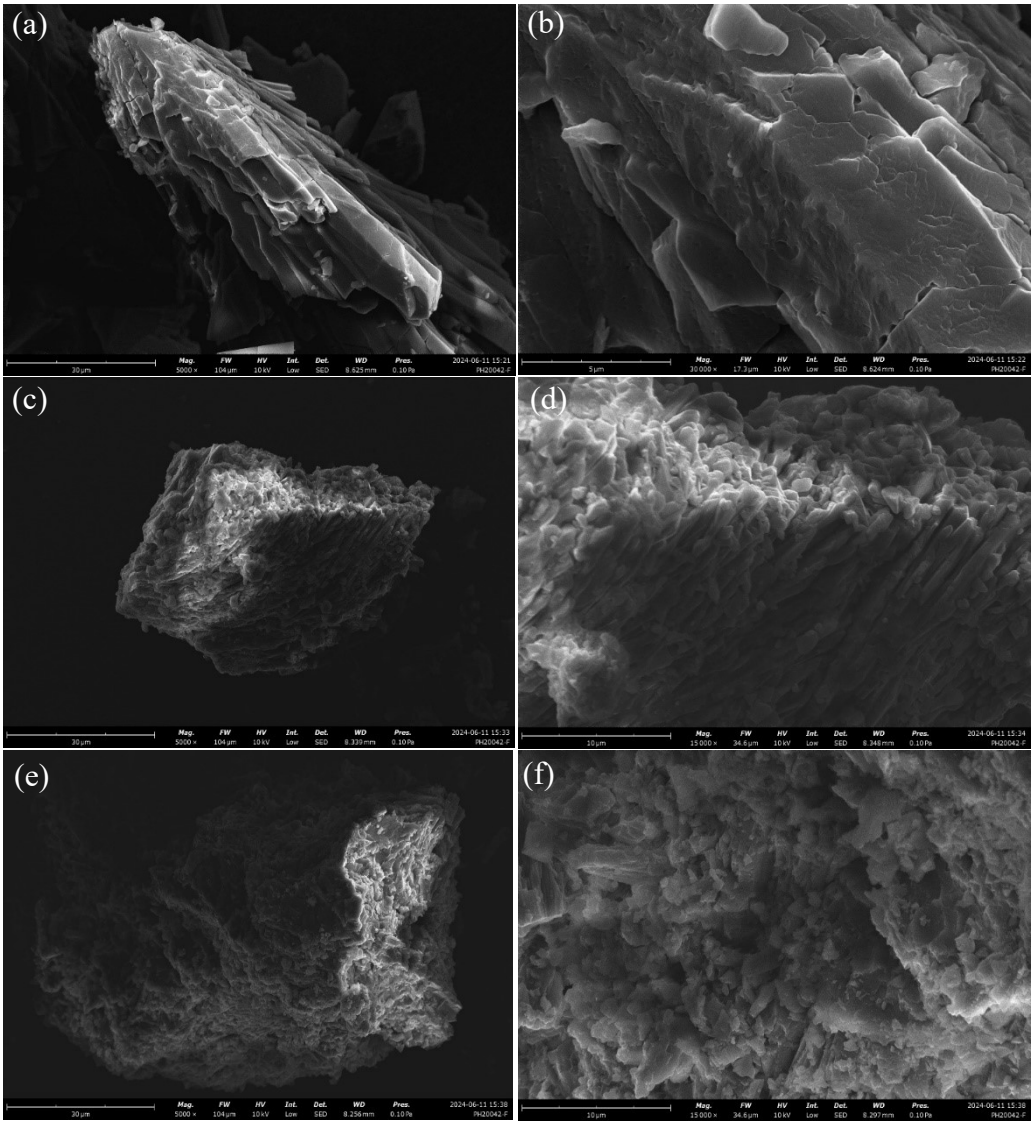

Fig. S1. SEM images of (a, b) Co-HOF; (c,d) Co9.5Ni0.5-HOF; (e, f) Co8Ni2-HOF.

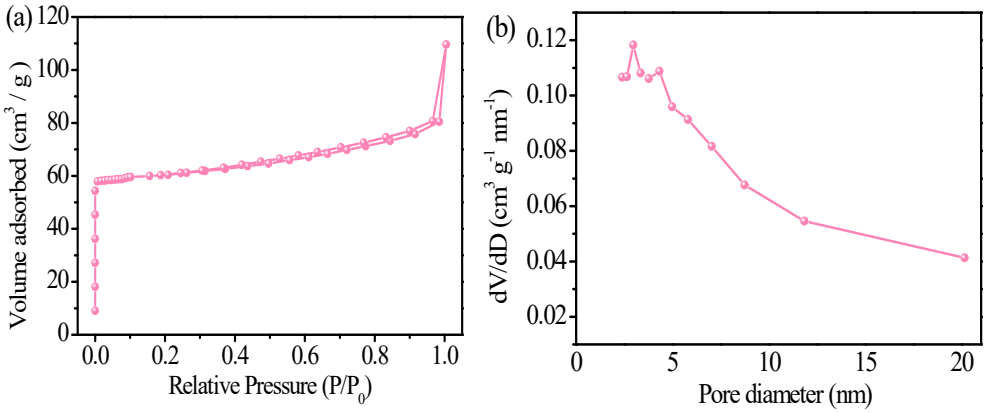

Fig. S2. (a) Nitrogen adsorption-desorption isotherms and (b) pore diameter distribution of Co-HOF.

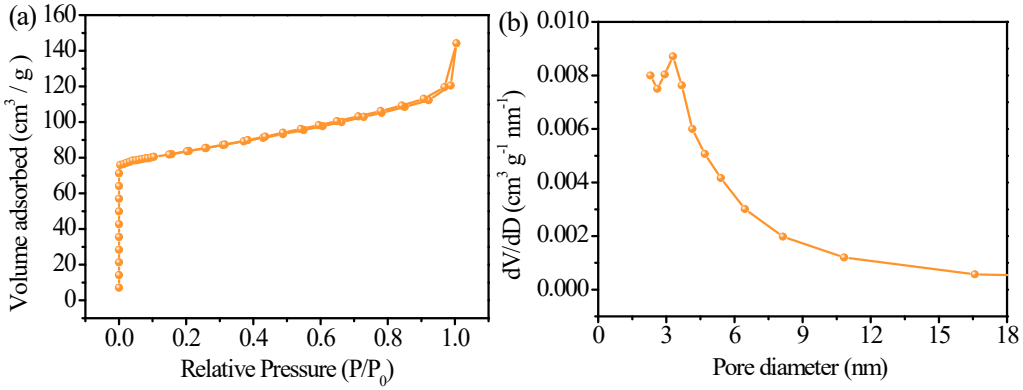

Fig. S3. (a) Nitrogen adsorption-desorption isotherms and (b) pore diameter distribution of $Co_{9.5}Ni_{0.5}$-HOF.

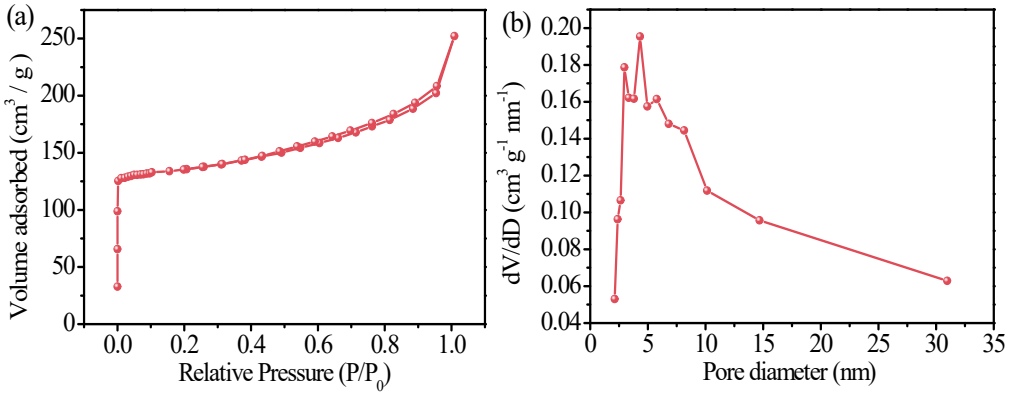

Fig. S4. (a) Nitrogen adsorption-desorption isotherms and (b) pore diameter distribution of Co_9Ni_1-HOF.

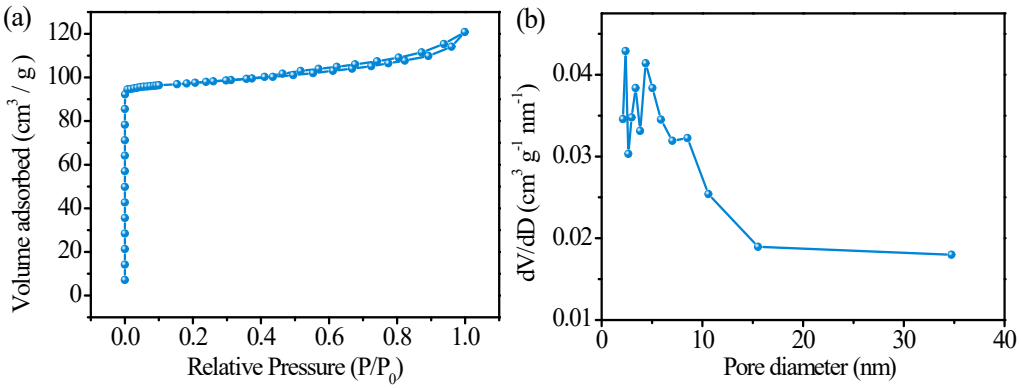

Fig. S5. (a) Nitrogen adsorption-desorption isotherms and (b) pore diameter distribution of Co_8Ni_2-HOF.

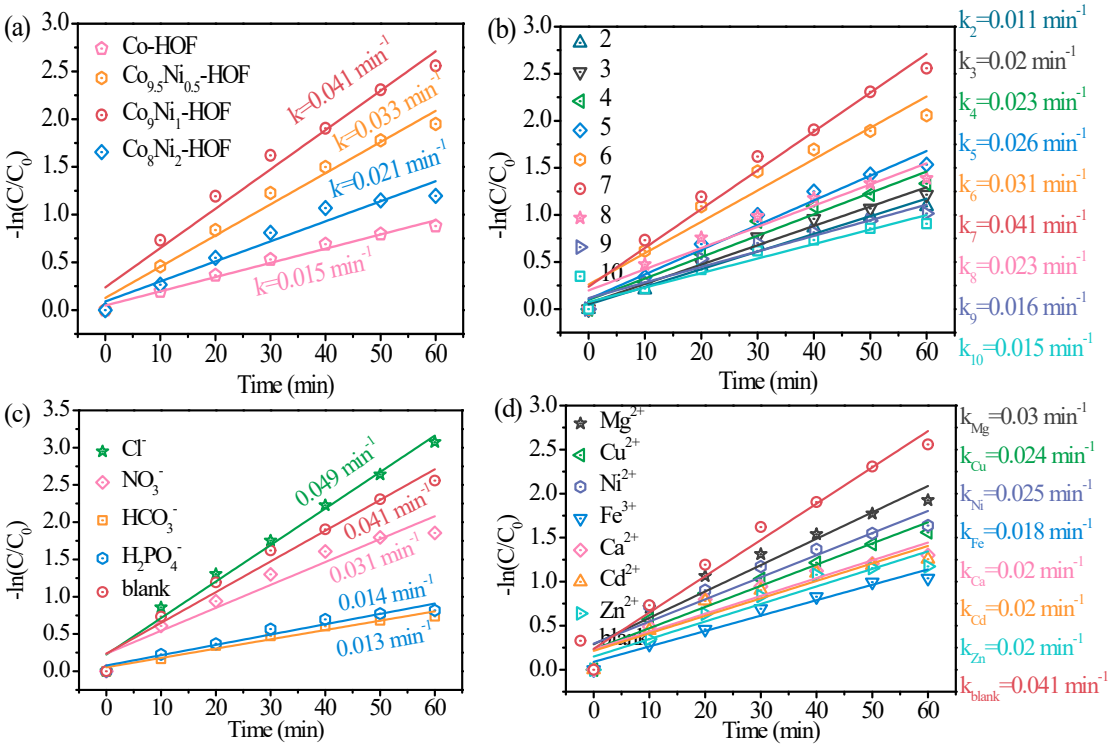

Fig. S6. (a) The kinetic rate constant of the UO_2^{2+} removal over different photocatalysts; (b-d) The kinetic rate constant of the UO_2^{2+} removal for different effects, (b) pH; (c) anions and (d) cations.

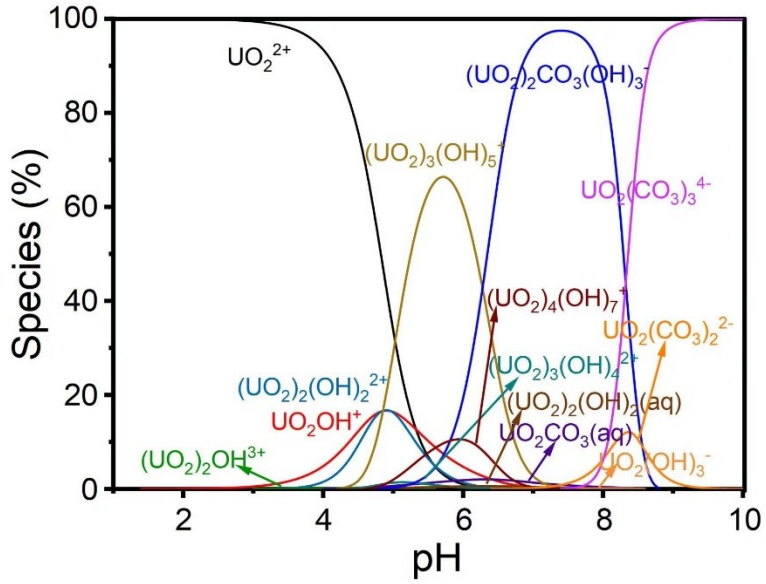

Fig. S7. Simulation of U(VI) speciation as a function with different pH.

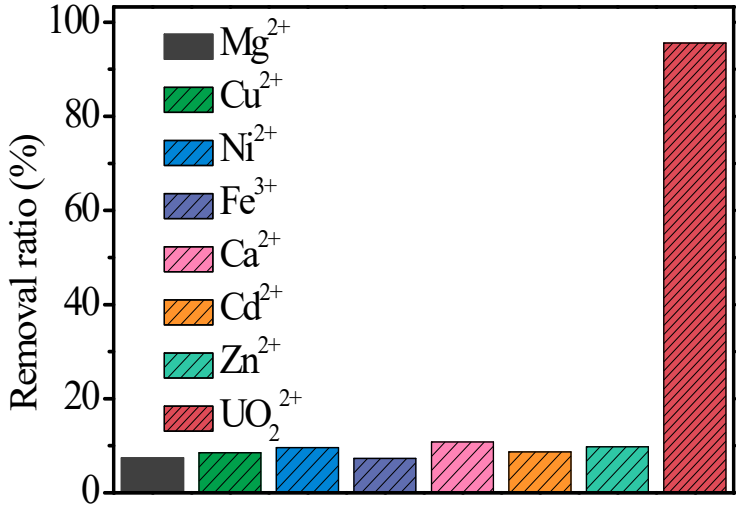

Fig. S8. Selective removal of coexistent ions on Co_9Ni_1-HOF.

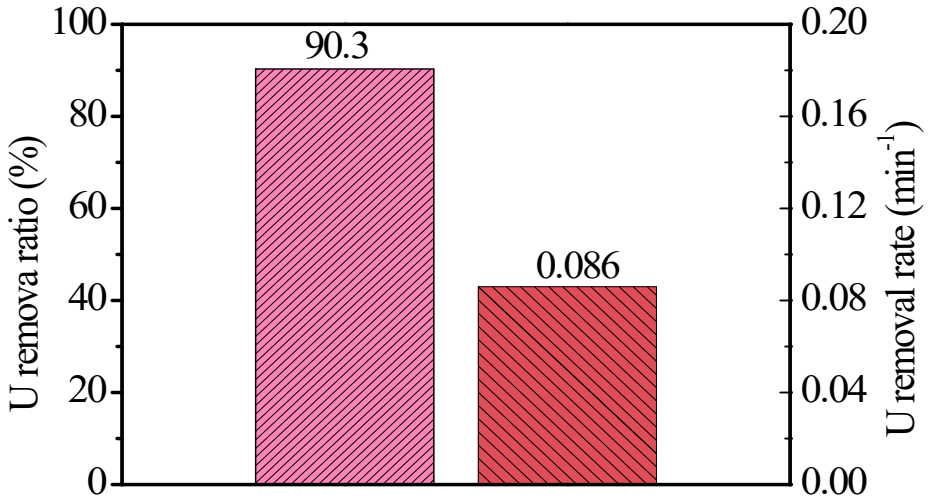

Fig. S9. The removal ratio and rate of U in simulated seawater for Co_9Ni_1-HOF photocatalyst

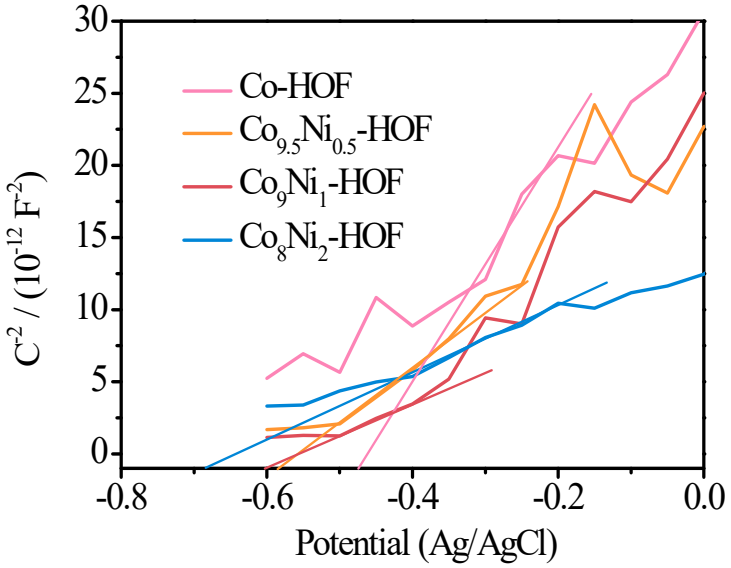

Fig. S10. Mott-Schottky plots of the various samples.

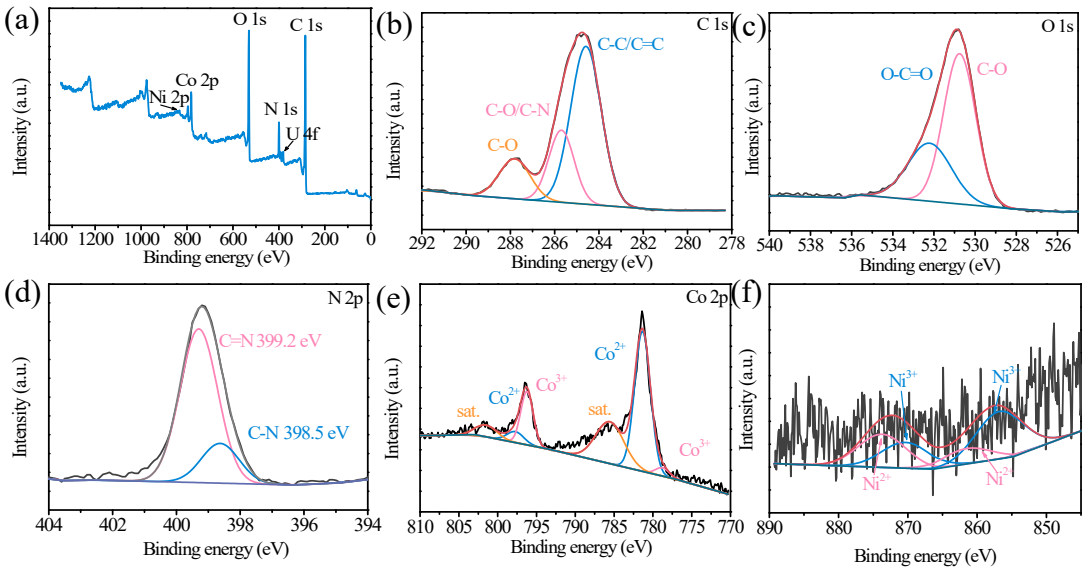

Fig. S11. (a) Full XPS region of Co_9Ni_1-HOF; high-resolution XPS spectra of (b) C 1s, (c) C 1s, (d) N 2p, (e) Co 2p and (d) Ni 2p after uranium removal.

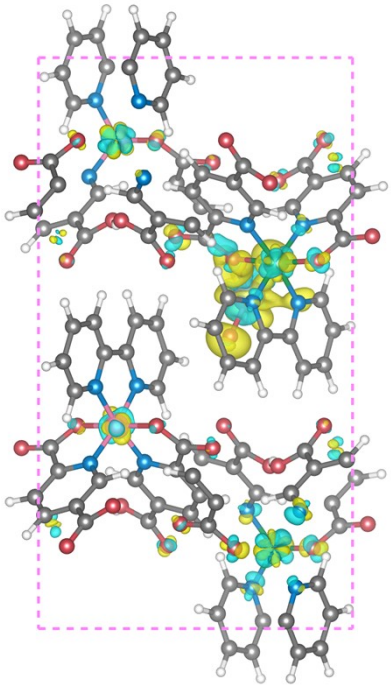

Fig. S12. Charge density differences of UO_2^{2+} adsorption on NiCo-HOF. Yellow indicates electron accumulation, and light blue indicates depletion.

Table S1. Surface and pore information of the samples.

Samples	Specific surface area (m^2/g)	Pore volume (cm^3/g)	Pore diameter (nm)
Co-HOF	191.62	0.137	2.4
$Co_{9.5}Ni_{0.5}$-HOF	308.34	0.192	2.83
Co_9Ni_1-HOF	432.66	0.364	3.67
Co_8Ni_2-HOF	270.85	0.185	2.86

Table S2. The ratio of different valence states over Co^{2+}/Co^{3+} and Ni^{3+}/Ni^{2+}

Samples	$Co^{2+}/Co^{3+}(2p_{1/2})$	$Co^{2+}/Co^{3+}(2p_{3/2})$	$Ni^{3+}/Ni^{2+}(2p_{1/2})$	$Ni^{3+}/Ni^{2+}(2p_{3/2})$
Co-HOF	1.006	1.018	-	-
Co_9Ni_1-HOF	1.008	1.021	1.002	1.003

Table S3. Comparison of HER activity with other materials.

Materials	Overpotential (mV)	Reference
$Mg_{0.99}Ni_{0.01}Ga_{0.01}Fe_{1.99}O_4$	-820	S1
2H-TaS_2	575	S2
Mo-doped SnS	377	S3
Ni-SAO	837.6	S4
Pd@TiO_2-H	430	S5
PSS (BiW@PEPS)	361	S6

B, P and S-doped Ag_2WO_4	330	S7
Ni/Ni_3C/CdS	-1080	S8
Cu-SnO_2/ZIF-8	364	S9
Cl-doped CuO	400	S10
MoS_2/BN/rGO	-422	S11
CuO Nanoflowers	1020	S12
Ag@g-C_3N_4/r-GO	484	S13
ZnO-Ti_3C_2	495	S14
$MnTiO_3$/g-C_3N_4	357	S15
$Co_{0.6}Cu_{0.4}Fe_2O_4$	-810	S16
Tetra-carboxylic acid based MOF	391	S17
Co_9Ni_1-HOF	355	This work

Reference:

[S1] R. Jasrotia, A. Verma, J. Ahmed, V. Khanna, M. Fazil, S. M. Alshehri, S. Kumari, P. Kumar, T. Ahmad, A. Kandwal, $Mg_{1-x}Ni_xGa_yFe_{2-y}O_4$ nano catalysts for green hydrogen generation with highly efffcient photo/electro catalytic water splitting applications, *Int. J. Hydrogen Energ*., 2024, **52**, 1228–1240.

[S2] E. Kovalska, P. K. Roy, N. Antonatos, V. Mazanek, M. Vesely, B. Wu, Zd. Sofer, Photocatalytic activity of twist-angle stacked 2D TaS_2, npj 2D Mater. Appl. 2021, **68**.

[S3] S. R. Kadam, S. Ghosh, R. Bar-Ziv, M. Bar-Sadan, Structural transformation of SnS_2 to SnS by Mo doping produces electro/photocatalyst for hydrogen production, *Chem. Eur. J*., 2020, **26**, 6679-6685.

[S4] C. L. Wang, H. Yang, J. Du, S. Z. Zhan, Catalytic performance of a square planar nickel complex for electrochemical- and photochemical-driven hydrogen evolution from water, *Inorg. Chem. Commun*. 2021, **131**, 108780.

[S5] C. Shu, H. Du, W. H. Pu, C. Z. Yang, J. Y. Gong, Trace amounts of palladium-doped hollow TiO_2 nanosphere as highly efficient electrocatalyst for hydrogen evolution reaction, *Int. J. Hydrogen Energ*. 2021, **46**, 1923-1933.

[S6] R. Manikandan, S. Sekar, S. P. Mani, S. Lee, D. Y. Kim, S. Saravanan, Bismuth tungstate-anchored PEDOT: PSS materials for high performance HER electrocatalyst, *Int. J. Hydrogen Energ*. 2023, **48**, 11746-11753.

[S7] M. M. Mohamed, M. Khairy, S. Eid, Phosphorous, boron and sulphur-doped silver tungstate-based nanomaterials toward electrochemical methanol oxidation and water splitting energy applications, *Int. J. Hydrogen Energ*. 2024, **50**, 1232–1245.

[S8] F. Y. Liu, F. Chen, X. Li, A. R. Xu, Z. J. Li, Z. J. Si, Z. Chen, A novel ternary nano-photocatalyst ($Ni/Ni_3C/CdS$) for HER and water purification with enhanced photocatalytic activity, *Chem. Eng. J.* 2023, **478**, 147242.

[S9] D. D. Zhang, H. M. Yang, Y. P. Li, Z. F. Li, N. Gao, W. J. Zhou, Z. H. Liang, High-performance Photoelectrocatalytic Reduction of CO_2 by the hydrophilic–hydrophobic composite Cu-SnO_2/ZIF-8, *Int. J. Electrochem. Sci.*, 2021, **16**, 150951.

[S10] D. P. Jaihindh, P. Anand, R. S. Chen, W. Y. Yu, M. S. Wong, Y. P. Fu, Cl-doped CuO for electrochemical hydrogen evolution reaction and tetracycline photocatalytic degradation, *J. Environ. Chem. Eng*. 2023, **11**, 109852.

[S11] S. Selvaraj, K. Natesan, P. B. Bhargav, A. Nafis, Revolutionizing water

treatment: Exploring the efficacy of MoS_2/BN/rGO ternary nanocomposite in organic dye treated water for OER and HER applications. *J. Water Process Engineering*, 2023, **54**, 104033.

[S12] F. Naaz, A. Sharma, M. Shahazad, T. Ahmad, Hydrothermally derived hierarchical CuO nanoflowers as an efficient photocatalyst and electrocatalyst for hydrogen evolution, *ChemistrySelect* 2022, **7**, e202201800.

[S13] S. R. Gujjula, U. Pal, N. Chanda, S. Karingula, S. Chirra, S. Siliveri, S. Goskula, V. Narayanan, Versatile bifunctional Ag@g-C_3N_4/r-GO catalyst for efficient photoand electrocatalytic H_2 production, *Energy Fuels* 2023, **37**, 9722−9735.

[S14] B. Saini, Harikrishna K, D. Laishram, R. Krishnapriya, R. Singhal, R. K. Sharma, Role of ZnO in ZnO nanoflake/Ti_3C_2 MXene composites in photocatalytic and electrocatalytic hydrogen evolution. *ACS Appl. Nano Mater*. 2022, **5**, 9319−9333.

[S15] F. Li, Y. Zhou, S. T. Xie, Z. L. Wu, Q. J. Wang, Y. N. An, H. H. Huang, Q. Y. He, F. Li, K. Y. Zhao, P. W. Wu, C. L. Yu, In-situ synthesis of 2D Z-scheme $MnTiO_3$/g-C_3N_4 heterostructure for efficient electrocatalytic hydrogen production, *J. Taiwan Inst. Chem. Eng.* 2023, **151**, 105085.

[S16] P. Kotwal, R. Jasrotia, A. V. Nidhi, J. Ahmed, S. Thakurf, A. Kandwal, M. Fazil, S. M. Alshehri, T. Ahmad, A. Verma, N. Sharma, R. Kumar, Photo/electro catalytic green hydrogen production promoted by Ga modified $Co_{0.6}Cu_{0.4}Fe_2O_4$ nano catalysts, *Environ. Res.* 2024, **241**, 117669.

[S17] Q. Qiu, T. Wang, L. H. Jing, K. Huang, D B. Qin, Tetra-carboxylic acid based metal-organic framework as a high-performance bifunctional electrocatalyst for HER

and OER, *Int. J. Hydrogen Energ.* 2020, **45**, 11077-11088.

Table S4. *k* values of the different samples.

Samples	Co-HOF	$Co_{9.5}Ni_{0.5}$-HOF	Co_9Ni_1-HOF	Co_8Ni_2-HOF
k values	0.0027	0.0047	0.0068	0.0031